



AMERICAN METEOROLOGICAL SOCIETY

Weather and Forecasting

EARLY ONLINE RELEASE

This is a preliminary PDF of the author-produced manuscript that has been peer-reviewed and accepted for publication. Since it is being posted so soon after acceptance, it has not yet been copyedited, formatted, or processed by AMS Publications. This preliminary version of the manuscript may be downloaded, distributed, and cited, but please be aware that there will be visual differences and possibly some content differences between this version and the final published version.

The DOI for this manuscript is doi: 10.1175/WAF-D-14-00070.1

The final published version of this manuscript will replace the preliminary version at the above DOI once it is available.

If you would like to cite this EOR in a separate work, please use the following full citation:

Peng, S., Y. Li, X. Gu, S. Chen, D. Wang, H. Wang, S. Zhang, W. Lv, C. Wang, B. Liu, D. Liu, Z. Lai, W. Lai, S. Wang, Y. Feng, and J. Zhang, 2015: A Real-Time Regional Forecasting System Established for the South China Sea and Its Performance in the Track Forecasts of Tropical Cyclones during 2011-13. *Wea. Forecasting*. doi:10.1175/WAF-D-14-00070.1, in press.



1 **A real-time regional forecasting system established for the**
2 **South China Sea and its performance in the track forecasts**
3 **of tropical cyclones during 2011-2013**

4 Shiqiu Peng^{1*}, Yineng Li¹, Xiangqian Gu², Shumin Chen¹,
5 Dongxiao Wang¹, Hui Wang³, Shuwen Zhang⁴, Weihua Lv⁵,
6 Chunzai Wang⁶, Bei Liu^{4,1}, Duanling Liu^{7,1}, Zhijuan Lai^{1,8},
7 Wenfeng Lai¹, Shengan Wang¹, Yerong Feng⁷, Junfeng Zhang⁸

- 8 1. State Key Laboratory of Tropical Oceanography, South China Sea Institute of
9 Oceanology, Chinese Academy of Sciences, Guangzhou 510301, China
10 2. State Key Laboratory of Severe Weather, Chinese Academy of Meteorological
11 Sciences, Beijing 100081, China
12 3. National Marine Environmental Forecasting Center, Beijing 100081, China
13 4. College of Ocean and Meteorology, Guangdong Ocean University, Zhanjiang
14 524088, China
15 5. Maoming Meteorological Bureau, Maoming 525000, China
16 6. NOAA/Atlantic Oceanographic and Meteorological Laboratory, Miami, FL 33149,
17 USA
18 7. Meteorological Center of Guangdong province, Guangzhou 510080, China
19 8. South China Sea Marine Prediction Center, the State Oceanic Administration,
20 Guangzhou 510310, China

21
22
23
24
25 Submitted to Weather and Forecasting

26 2014. 12. 28

27

* Corresponding author: Dr. Shiqiu Peng, 164 West Xingang Road, LTO/SCSIO, Guangzhou, 510301, China
Email: speng@scsio.ac.cn

Abstract

28

29 A real-time regional forecasting system for the South China Sea (SCS), called the
30 experimental platform of marine environment forecasting (EPMEF), is introduced in
31 this paper. EPMEF consists of a regional atmosphere model, a regional ocean model
32 and a wave model, and performs real-time run four times a day. The output of the
33 Global Forecasting System (GFS) from the U.S. National Centers for Environmental
34 Prediction (NCEP) is used as the initial and boundary conditions of two nested
35 domains of the atmosphere model which can exert constraint on the development of
36 small- and meso-scale atmospheric perturbations through dynamical downscaling.
37 The forecasted winds at 10-m height from the atmosphere model are used to drive the
38 ocean and wave models. As an initial evaluation, a census on the track predictions of
39 44 tropical cyclones (TC) in 2011-2013 indicates that the performance of EPMEF is
40 very encouraging and comparable to those of other official agencies worldwide. In
41 particular, EPMEF successfully predicted several abnormal typhoon tracks including
42 the sharp recurving of Megi (2010) and the looping of Roke (2011). Further analysis
43 reveals that the dynamically downscaled GFS forecasts from the most updated
44 forecast cycle and the optimal combination of different microphysics and PBL
45 schemes primarily contribute to the good performance of EPMEF in TC track forecast.
46 EPMEF, established primarily for research purpose with potential to implement into
47 operation, provides valuable information not only to the operational forecasters of the
48 local marine/meteorological agencies or the international TC forecast centers, but also
49 to other stake-holders such as fishing industry and insurance companies.

50 **1. Introduction**

51 Being the largest tropical marginal sea and connecting the western Pacific Ocean
52 and the eastern Indian Ocean, the South China Sea (SCS) plays an important role in
53 the exchange of water mass and energy between the two ocean basins (Qu et al. 2005;
54 Qu and Du 2006; Wang et al. 2006; Du and Qu 2010). It is also an area where tropical
55 cyclones (TC) or typhoons form and pass in the summer and fall seasons, which
56 causes huge damage of property and loss of life in the East Asian countries such as
57 Philippines, Vietnam and China (Wu and Kuo 1999). For instance, about 7-8 typhoons
58 make landfall in China per year, impacting a population of 250 million with property
59 loss of over 10 trillion dollars (Liu et al. 2009).

60 Although the forecasts of the tropical cyclone track or intensity have been
61 improved during the past several decades, large uncertainties still exist. This is due to
62 the poor understanding of physical processes about tropical cyclone intensity as well
63 as the inherent predictability limit in numerical models which still fall short in
64 capturing the intricacies of the underlying mechanisms (Fraedrich and Leslie 1989;
65 Plu 2011; Peng et al. 2013). Besides high-quality initial conditions (Kurihara et al.
66 1995; Leslie et al. 1998; Bender et al. 2007), factors contributed to improve the TC
67 forecasting accuracy of a model may include: the domain settings regarding to size
68 and location (Landman et al. 2005; Giorgi 2006), the choice of horizontal resolutions
69 for the nested domain, the selected microphysics parameterization scheme (Rao and
70 Prasad 2007, Kanada et al. 2012, Kepert 2012) or/and Planetary Boundary Layer
71 (PBL) parameterization scheme (Khain and Lynn 2011, Pattanayak et al. 2012) as

72 well as their combination (Zhou et al. 2013), and so on. This paper introduces a
73 real-time regional forecasting system established for the SCS whose atmosphere
74 model features with two nested domains centered in the SCS, a "dynamical
75 downscaling" initialization scheme and an "optimal" combination of the Ferrier
76 microphysics scheme and the YSU PBL scheme, and presents a preliminary
77 evaluation of its performance in TC track forecasts during 2011-2013.

78 The paper is organized as follows. Section 2 gives a brief description to the
79 establishment of the real time forecasting system. An evaluation of the performance of
80 the forecasting system in TC track forecasts is presented in Section 3, followed by a
81 detailed a discussion in Section 4. A summary is given in the final section.

82

83 **2. Establishment of EPMEF**

84 A real-time air-sea-wave forecasting system for the SCS, also named experimental
85 platform of marine environment forecasting (EPMEF), was established in the State
86 Key Laboratory of Tropical Oceanography (LTO), South China Sea Institute of
87 Oceanology (SCSIO) in Oct. 2010. It consists of three main components, i.e., an
88 atmospheric model, an ocean model and a sea wave model, which are the Weather
89 Research and Forecasts (WRF) model Version 3.2 (Michalakes et al. 1998;
90 Skamarock et al. 2008), the Princeton Ocean Model (POM) 2002 version (Blumberg
91 and Mellor 1987; Mellor et al. 2003) and the WAVEWATCH III (WW III) model
92 (Tolman 1997, 1999, 2002), respectively. Fig. 1 shows the flow chart of EPMEF.

93 The WRF model (Version 3.2), developed by the National Center for Atmospheric
94 Research (NCAR) and the National Centers for Environmental Prediction (NCEP) in
95 the U. S., is a next-generation meso-scale numerical weather prediction system that
96 was designed to serve both operational forecasting and atmospheric research needs
97 (Michalakes et al. 1998; Skamarock et al. 2008). Dynamical downscaling techniques
98 are commonly used for a regional atmospheric model to obtain higher-resolution
99 output with small- and meso-scale features from the lower-resolution output of a
100 global atmospheric model (Lo et al. 2008; Zhang et al. 2009). To realize this, a
101 two-domain-one-way-nested configuration is designed, as shown in Fig. 2. The outer
102 domain for the atmospheric model covers the western Pacific Ocean, the entire SCS,
103 and the eastern Indian Ocean, with a horizontal grid resolution of 72 km. The inner
104 domain covers the entire SCS and southern China, with a horizontal grid resolution
105 of 24 km. Both domains have 27 layers in the vertical. The horizontal resolutions of
106 72 km (outer domain) and 24 km (inner domains) and 27 vertical layers are chosen
107 mainly due to the limited computer resources (currently EPMEF is running in a Rack
108 Server with 32 cores of Intel Xeon E5 with 2.6 Hz), and they can be updated to
109 higher resolutions in the future when more computer resources are available. The
110 output from the Global Forecast System (GFS) maintained by NCEP with horizontal
111 grid resolution of $1^{\circ}\times 1^{\circ}$ is used to provide initial conditions (IC) and lateral
112 boundary conditions (BC) for the outer domain. The Ferrier microphysics scheme
113 (Ferrier et al. 2002), Kain-Fritsch cumulus scheme (Kain and Fritsch 1990, 1993),
114 YSU PBL scheme (Hong et al. 2006), and Dudhia short wave (Dudhia 1989) and

115 RRTM long wave (Mlawer et al. 1997) radiation scheme are chosen for both
116 domains. A 15-day forecasting and a 3-day forecasting are made automatically every
117 6 hours (i.e., 4 times a day at 0200, 0800, 1400, 2000 Beijing time) for the outer and
118 inner domains, respectively.

119 The 10-m height winds from the inner domain of WRF model are used to drive the
120 ocean model POM (2002 version) and the wave model WW III. POM is a
121 three-dimensional (3-D) ocean model with primitive equations, embedded a second
122 moment turbulence closure model (the 2.5 Mellor-Yamada scheme; Mellor and
123 Yamada, 1982). The WW III model is a third generation wave model developed at
124 NOAA/NCEP (Tolman, 1997, 1999, 2002). As the an initial evaluation of EPMEF,
125 we focus on the performance of EPMEF in the TC track forecasts in this paper, and
126 thus here we omit the detailed descriptions of the set up for the ocean model and
127 wave model. The evaluation for the performance of the ocean and wave models will
128 be given in our future publication once enough observations are available.

129

130 **3. Evaluation of the performance in TC track forecasts during 2011-2013**

131 The SCS and the western Pacific Ocean are the regions affected by typhoons or
132 tropical storms most frequently in summer and autumn. For instance, there are 77
133 named and numbered tropical storms/typhoons occurring in these areas during
134 2011-2013. Therefore, as an initial evaluation of the performance of EPMEF, we
135 focus on the track forecasts of tropical cyclones during 2011-2013 by EPMEF and
136 make comparison with the forecasts by other major agencies, including the U.S.

137 Navy/Air Force Joint Typhoon Warning Center (JTWC), the Japan Meteorological
138 Administration (JMA), the National Meteorological Center of China (NMCC), and
139 the Central Weather Bureau of Taiwan (CWBT). Since 2012 TC season, the
140 Environmental Modelling Center (EMC) of the National Center of Environment
141 Prediction (NCEP) in U.S. began to make real-time forecasts for West Pacific TCs
142 using HWRF model (Tallapragada et al. 2013), thus we also compare our results of
143 2012-2013 TC forecasts with those from NCEP/EMC. Due to limited computer
144 resources, EPMEF only makes 72-h track forecasts for TCs entering the inner
145 domain. TC vortexes are initialized by downscaling the “first guess” from GFS in 1°
146 $\times 1^\circ$ resolution to regional model WRF in 24-km resolution. There are 21, 25 and 31
147 named tropical cyclones in 2011, 2012 and 2013, respectively. For all of these TCs,
148 only those that entered the inner domain of the atmospheric model of EPMEF with
149 life cycle longer than 48 hours and were forecasted by at least 3 other agencies are
150 counted in our statistics, which results in a count of 10, 16 and 18 TCs for 2011,
151 2012 and 2013, respectively. As an example, Fig. 2 shows the tracks of the 18 TCs
152 for 2013 that entered the inner domain with life cycle longer than 48 hours. The TC
153 center is tracked by a routine of position search available in the WRF post-process
154 program RIP4, which takes into account the criteria in both upper atmosphere and
155 sea surface: the predicted minimum sea level pressure, maximum 10-m height winds,
156 maximum vorticity at 650 hPa and 850 hPa, as well as some prescribed thresholds
157 for the vorticity at all levels and the temperature at surface and 700 hPa. Based on
158 the observed track (“best” track) issued by JTWC, the track position errors (TPE) for

159 24-h, 48-h and 72-h forecasts by each agency are calculated using the following
 160 formula (Neumann and Pelissier 1981; Powell and Abernson 2001):

$$161 \quad TPE = 111.11 \frac{180}{\pi} \cos^{-1} \left[\sin \phi_0 \sin \phi_s + \cos \phi_0 \cos \phi_s \cos (\lambda_0 - \lambda_s) \right], \quad (1)$$

162 where λ_0 and ϕ_0 are longitude and latitude of the storm center in the best track
 163 data, and λ_s and ϕ_s are those of the forecasted storm center from each agency. To
 164 make a relatively fair comparison among the agencies, we calculate the relative
 165 errors of each TC track predicted by each agency using the following formula:

$$166 \quad R_i = TPE_i / \overline{TPE} \quad (i=1, \dots, N), \quad (2)$$

167 where $\overline{TPE} = \frac{1}{N} \sum_{i=1}^N TPE_i$ and N denotes the number of agencies. If an agency has
 168 no forecasting result available for a TC, 1.0 is assigned to it. It is obvious that, the
 169 smaller the value of R_i is, the better the corresponding agency performs. We define
 170 the relative forecasting skill as the mean of R_i of all TCs for each agency for 24-h,
 171 48-h and 72-h forecasts, respectively.

172 Figs. 3-5 give the mean TPE of and the relative error R_i of 10, 16 and 18 TCs for
 173 2011, 2012 and 2013, respectively. The mean TPE (R_i) over the 10 TCs in 2011
 174 from EPMEF reads 97.0 km (0.98), 172 km (1.05) and 278 km (1.0) for 24-h, 48-h
 175 and 72-h forecasting, respectively, ranking the third, the fourth and the second
 176 among the five agencies. In 2012 and 2013, the forecasts from NCEP-HWRF are
 177 available for comparison besides the other four agencies. The mean TPE (R_i) from
 178 EPMEF reads 83 km (0.87), 133 km (0.85) and 232 km (0.95) for the 16 TC in 2012
 179 (ranking the 1st, 1st, and 2nd) and 86 km (0.98), 129 km (0.87) and 171 km (0.90) for
 180 18 TC in 2013 (ranking the 3rd, 1st and 1st) for 24-h, 48-h and 72-h forecasting,

181 respectively. As examples, Figs. 6-7 show the performance of each agency for
182 Nanmadol (2011) and Rumbia (2013) which made landfall on the coasts of Jinjiang,
183 Fujian province and Zhanjiang, Guangdong province, respectively. For Nanmadol
184 (2011), EPMEF performed slightly better than others for the 24-h forecast with a
185 mean TPE of 84 km, although the TPE increased quickly at the last initialization
186 time (0000 UTC 30 Aug. 2011) probably due to initialization quality associated with
187 the accuracy of the GFS forecasts at that time when the TC was going to make
188 landfall. EPMEF performed significantly better than others for the 48-h and 72-h
189 forecasts with a mean TPE of 137 km and 289 km, respectively, especially for the
190 second half of the period. The 72-h predicted track by EPMEF initializing at 1200
191 UTC 27 Aug. 2011 is very close to the observed one (Fig. 6d). For Rumbia (2013),
192 EPMEF performed much better than others with a mean TPE of 53 km, 64 km and
193 129 km for the 24-h, 48-h and 72-h forecasts, respectively. As indicated in Fig. 7d,
194 initializing at 0000 UTC 29 Jun. 2013, the EPMEF predicted a track and a landfall
195 location three days ahead which are very close to the observations. In contrast,
196 EPMEF shows the worst performance in some TCs, such as the strong typhoon
197 Netsat (2011), of which large TPEs for all forecast times are seen for EPMEF (Fig.
198 8). In an overall assessment for the three TC seasons of 2011-2013, the performance
199 of EPMEF is very encouraging compared to those of some official agencies.

200 Now let us look into a couple of cases that have “abnormal” tracks and are most
201 difficult to be predicted: Megi (2010) and Roke (2011). Megi (2010) is the strongest
202 typhoon in the world in 2010 and the strongest one generated in western Pacific

203 Ocean at autumn in the past 20 years, with maximum wind speed of 72 m/s and
204 lowest sea level pressure of 895 hPa. The most astonishing feature of its track is its
205 nearly 90-degree turn from westward to northward at 0000 UTC 20 Oct. 2010 after it
206 passed through Philippines and entered the SCS. Most of the official agencies did
207 not predict this “big turn” until 2100 UTC 19 Oct. 2010. EPMEF, however,
208 successfully predicted the “big turn” as early as 0000 UTC 18 Oct. (Fig. 9a). As
209 revealed by Peng et al. (2014), the cold air intrusion from the northwest played a key
210 role in the “big turn” of Megi (2010) through adjusting the large scale circulation.
211 The cold air intrusion was well predicted by EPMEF, mainly attributed to the proper
212 selection of PBL and physical schemes as indicated by Zhou et al. (2013) and
213 discussed in Subsection 4.2. Roke (2011) generated as a tropical storm in the
214 location (137°E, 22.1°N) of the western Pacific at 1200 UTC 13 Sep. 2011, when it
215 moved westward to the east of Okinawa Island (129.7°E, 26.4°N) at 0600 UTC 16
216 Sep., it turned around and looped cyclonically and intensified to a typhoon; after the
217 looping, it moved northward and then northeastward, and made landfall on Shizuoka
218 county of Japan at 0600 UTC 21 Sep. 2011. As early as 1200 UTC 14 Sep. 2011,
219 EPMEF successfully predicted the cyclonical loop that is usually very hard to predict
220 (Fig. 9b). Figs. 9c-d show the 48-h and 72-h TPE of Roke (2011) for each
221 forecasting agencies (forecasting data from JTWC are not available), in which the
222 performance of EPMEF is seen very encouraging with a minimum mean 48-h TPE
223 of 130.15 km and 72-h TPE of 194.03 km, compared to the mean 48-h TPE of 241.3

224 km, 195.8 km, 219.6 km and 72-h TPE of 342.7 km, 304.4 km, 340.9 km for NMCC,
225 JMA and CWBT, respectively.

226

227 **4. Discussion**

228 4.1 The initialization process

229 The above results indicate that the performance of EPMEF appears comparable to
230 or even better than most of the official agencies. However, one should be aware the
231 following points: 1) the comparison is based on only those TCs that entered the inner
232 domain of EPMEF and lasted longer than 48 h in the domain; 2) the track forecasts
233 from EPMEF are purely from its numerical model initialized at the starting time of
234 the current forecast cycle, but those released online by the official agencies are
235 usually based on results from a number of guidance models including multi-layer
236 dynamical models, single-layer trajectory models, consensus models, and statistical
237 models, as well as the experiences of forecasters. Therefore, the comparison here is
238 not the one purely among numerical models. Guidance models are characterized as
239 either early or late, depending on whether or not they are available to forecasters
240 during the forecast cycle. For example, the GFS forecasts made for the 1200 UTC
241 forecast cycle would be considered a late model since it is not complete and
242 available to forecasters until about 1600 UTC, or about an hour after the NHC
243 forecast is released, i.e., it could not be used to prepare the 1200 UTC official
244 forecast. Multi-layer dynamical models are generally, if not always, late models. To
245 make the forecast benefit from a late model as much as possible while keep it timely,

246 a technique is adopted which adjusts the most recent available run of a late model to
247 the current synoptic time and initial conditions. The adjustment process produces an
248 “early” version of a late model for the current forecast cycle that is based on the
249 most current available guidance. The adjusted version of a late model is known,
250 mostly for historical reasons, as “interpolated” model. Since the initial and boundary
251 conditions in the real atmosphere may vary significantly at different time, the
252 forecast of a dynamical (late) model starting from previous forecast cycle (i.e.,
253 initializing at 0600 UTC or 0000 UTC) for the current forecast cycle (1200 UTC)
254 (on which the “interpolated” model is based) is generally less accurate than that
255 starting from the current forecast cycle (i.e., initializing at 1200 UTC). This may be
256 the main reason why the forecasts of EPMEF are generally more accurate than those
257 of most official agencies based on “interpolated” models. However, EPMEF
258 achieves this in a cost of about 2-h late release of forecasts. For instance, at the 1200
259 UTC forecast cycle, EPMEF waits until 1515 UTC for the coming of GFS forecasts
260 initializing at 1200 UTC which are not available until 1500 UTC. Running in a Rack
261 Server with 32 cores of Intel Xeon E5 with 2.6 Hz, it generally takes about one and
262 half an hour for EPMEF to download the GFS data, prepare IC/BC and finish a 72-h
263 forecasting, so the track forecast from EPMEF could be released at about 1630UTC,
264 i.e., one and half an hour late compared to the forecast release time (1500 UTC) by
265 the official agencies. For forecasts longer than 24 hours, the negative impact of a 2-h
266 delay of forecast release is nearly negligible. Thus, in our opinion, it is worth to gain
267 an improvement for TC track forecasts in the cost of about one or two hours delay of

268 forecast release (the delaying time may be shortened to less than one hour if a faster
269 computer is used in the future), especially for a forecast period of longer than 24
270 hours.

271 To see how EPMEF may benefit from using the GFS forecasts of the current
272 forecast cycle (i.e., the “late model”) to create IC/BC, we perform an ensemble of
273 hindcasts for the 16 TCs of 2012 using a different initialization scheme to create
274 IC/BC (denoted as EPMEF-6). The initialization scheme for EPMEF-6 uses GFS
275 forecasts of the previous forecast cycle (6-h early) for generating IC/BC, which is
276 similar to the “early model” except that it does not carry out any adjustment or
277 projection to the GFS forecasts of the previous forecast cycle. For EPMEF-6, the
278 mean TPEs for 24-h, 48-h and 72-h forecasts are 96.6 km, 159.4 km, and 270.3 km,
279 respectively, an apparent degrade compared to those of 82.8 km, 133.4 km, and
280 232.3 km for EPMEF (Fig. 4). Therefore, the reduction of TPEs in EPMEF is
281 obviously attributed to a better representation of the initial large-scale environmental
282 circulations in the “late model”. The adjustment or projection according to the latest
283 information of the live TC implemented in the standard “early model” is believed to
284 improve the small- and meso-scale features of the meteorological fields in the
285 regional model, but may not be much helpful on improving the large-scale
286 environmental circulations which steer the TC. Fig. 10 displays the steering flows
287 and the 500-hpa potential height from EPMEF and EPMEF-6 for the typhoon Gaemi
288 (2012) at the initialization time of 1200 UTC 3 Oct. 2012 and 30-h forecast time,
289 imposed by the TC best track and the simulated tracks. The steering flows are

290 obtained through averaging the wind field between 925 hPa and 300 hPa and over a
291 3~8° radial band centered at the TC eye, based on the suggestions or experiences in
292 some studies (Chan and Gray 1982; Dong and Neumann 1983). Although the initial
293 vortex position from EPMEF-6 is a little bit closer to the one from the best track than
294 that from EPMEF, the northward component of steering flows from EPMEF-6
295 makes the cyclone move to the north, while the southward component of steering
296 flows from EPMEF drives the cyclone to the south which is closer to the best track.
297 The field of geopotential height in EPMEF also appears to be in favor of a
298 southwestward movement of the cyclone, while that in EPMEF-6 seems to facilitate
299 the northeastward movement which deviates from the observed track of the cyclone.
300 The biases of u- and v-components of steering flows from the 72-h forecasts of
301 EPMEF and EPMEF-6 against the FNL analysis are displayed in Fig. 11, which are
302 averaged over an ensemble of model runs initialized at every 6-h from 0000 UTC 2
303 Oct. to 1200 UTC 5 Oct. 2012. Significant reduction of biases in the v-component of
304 steering flows is found for EPMEF, implying that the “late model” used in the
305 initialization of EPMEF can better capture the large-scale environmental circulations
306 not only in the initial time but also in the forecasting times. Therefore, EPMEF
307 benefits from the GFS forecasts of the current forecast cycle (the most updated)
308 which bring a better steering flow than those of the previous forecast cycle (6-h
309 early), leading to better track forecasts of TCs.

310

311 4.2 The effect of microphysics and PBL schemes

312 Another important factor contributed to the good performance of EPMEF could be
313 the choice of the Ferrier microphysics scheme and the YSU Planetary Boundary
314 Layer (PBL) scheme in the model. As shown in the study of Zhou et al. (2013),
315 various combinations of microphysics schemes and PBL schemes may have different
316 influence on TC track simulation, and the combination of Ferrier scheme and YSU
317 scheme is the “optimal” one that leads to a best track simulation of super typhoon
318 Megi (2010). The influence of various combinations of the microphysics schemes
319 and PBL schemes on TC track forecasts may depend on the model configuration
320 such as the horizontal grid resolution, the domain size and topography, etc.. To
321 investigate their influences on TC track forecasts in the configuration of EPMEF, we
322 carry out a number of experiments using different combinations of four microphysics
323 schemes (i.e., Ferrier, Goddard, WSM6, and Lin, see a detailed description in
324 Skamarock et al. 2008) and three PBL schemes (i.e., YSU, MYJ, and MYNN2, see a
325 detailed description in Skamarock et al. 2008) and initializing at every 6 hours from
326 1200 UTC 21 Jul. to 1800 UTC 23 Jul. for the typhoon Vicente (2012). The mean
327 TPEs for various combinations are given in Table 1. It is found that the combination
328 of Ferrier scheme and YSU scheme has the smallest mean TPE for both 24-h and
329 72-h forecasts. Although the combinations of the MYJ PBL scheme with most
330 microphysics schemes performs well, they do not work (blow up) for the 72-h
331 forecast. Therefore, in an overall assessment, the combination of Ferrier scheme and
332 YSU scheme performed the best among all combinations, as indicated by the rank
333 based on the sum of relative errors of all forecast periods for each combination

334 (Table 1). This can be attributed to a more accurate forecasting of the large-scale
335 environmental circulations (i.e., the steering flows) from the combination of Ferrier
336 scheme and YSU scheme as indicated in Fig. 12. Considering the influence of
337 various combinations may be case-dependent in the configuration of EPMEF, we
338 have carried out an ensemble of experiments using different combinations of
339 microphysics schemes and PBL schemes for a number of typhoon cases. The results
340 also show that the combination of Ferrier scheme and YSU scheme produces a more
341 accurate forecasting of the steering flows which are governed by the large scale
342 circulations, leading to better TC track forecasts (figures not shown). Hence, EPMEF
343 benefits obviously from the choice of the Ferrier microphysics scheme and the YSU
344 PBL scheme, resulting in a better performance in TC track forecasts.

345

346 4.3 Other factors influencing the performance of EPMEF

347 There may be other factors influencing the performance of EPMEF, such as the
348 domain settings regarding to size and location, the choice of horizontal resolutions
349 for the nested domain, and so on. As indicated in the study of Landman et al. (2005),
350 model domain choice is important in the simulation of TC-like vortices in the
351 southwestern Indian Ocean. Giorgi (2006) also pointed out that one should carefully
352 consider the choice of domain size and location in relation to model resolution and
353 the placement of domain boundaries in the design of regional climate simulation
354 experiments. Nevertheless, the results from a set of experiments with different
355 domain sizes and location (shifting the domain to the east or west) as well as an

356 increased resolution (from 24 km to 10 km in the inner domain) indicate that, though
357 differences among these experiments exist, they are relatively small compared to
358 those among different combination of PBL and microphysics schemes (figure
359 omitted). Considering both the model performance and the computation cost, the
360 current model configuration regarding the domain sizes and location as well as
361 horizontal resolution are thus nearly optimal. With more computer resources
362 available in the future, we will update the current horizontal resolution of EPMEF to
363 a higher one (say, 10km in the inner domain) which we believe will benefit the
364 performance of EPMEF.

365 It is obvious that the EPMEF performed much better for the 2012 and 2013 TC
366 seasons than for the 2011 TC season in TC track forecasts. The better performance of
367 the EPMEF could attributed to the following factors: 1) the large-scale forecasts
368 from GFS are probably improved in the 2012-2013 TC seasons compared to those in
369 the 2011 one due to the use of ensemble forecast information as background error
370 estimation in NCEP GSI through the hybrid ensemble-GSI system, which in turn
371 improves the IC/BC in EPMEF and results in more accurate TC track forecasts for
372 the 2012-2013 TC seasons; 2) the network for EPMEF was updated with higher
373 speed since 2012, which allows more most-updated GFS data to be downloaded
374 before the starting of the model run for each forecast cycle in the 2012-2013 TC
375 seasons than in the 2011 one. As demonstrated in Subsection 4.1, the performance of
376 EPMEF can benefit from the most updated GFS forecast.

377

378 **5. Summary**

379 A real-time air-sea-wave regional forecasting system for the SCS has been
380 established. It consists of a regional atmosphere model WRF, a regional ocean model
381 POM and a sea wave model WW III. The output from the Global Forecasting
382 System (GFS) of NCEP is used as the initial conditions and boundary conditions of
383 WRF which exerts constraint on the development of small and meso-scale
384 atmosphere perturbations through dynamical downscaling in two nested domains.
385 The wind field at 10-m height forecasted by WRF is used to drive the ocean model
386 and the sea wave model. The preliminary results from its near real-time run (four
387 times a day) for the last three years demonstrate that it is stable and reliable under
388 various situations. In particular, the performance of EPMEF in typhoon track
389 prediction during 2011-2013 TC seasons is very encouraging compared to other
390 major agencies in the world, although in a cost of about two-hour delay of forecast
391 release. The dynamically downscaled GFS forecasts from the most updated forecast
392 cycle and the optimal combination of different microphysics and PBL schemes
393 primarily contribute to the good performance of EPMEF in TC track forecast.

394 EPMEF, established primarily for research with proven capability and reliability
395 to apply into operational, can provide not only valuable references to the forecasters
396 of the local official marine and meteorological forecast agencies in their daily
397 operational forecasts, but also some practical clues or hinds for improving TC
398 forecast skills to the world-wide official forecast agencies. Moreover, it has also
399 played a role in serving for some important social activities and scientific marine

400 surveys in the SCS and its surrounding regions by providing the necessary
401 environmental forecasts (especially the TC track forecast) with relatively high
402 accurateness since its establishment.

403 EPMEF, however, is still under continuously developing and improving. In the
404 future, a three-way-interactive air-sea-wave coupled system will replace the current
405 one-way-down-stream one, with a higher grid resolution for the atmospheric
406 component. Furthermore, data assimilation package will be incorporated into
407 EPMEF for assimilating both the atmospheric and oceanic observations (including
408 in-situ and satellite-derived observations) using 3-dimensional and 4-dimensional
409 variational data assimilation approaches (3DVAR/4DVAR). In particular, a
410 “scale-selective data assimilation” (SSDA) scheme (Peng et al. 2010) will be
411 employed to assimilate the large-scale atmospheric circulation from the forecasts of
412 a global model into WRF for improving the track prediction of tropical cyclones
413 (Xie et al. 2010). It is expected that, the TC track forecasts by EPMEF will be
414 improved in the coming future. On the other hand, the forecasts of storm surges and
415 waves from the ocean and wave model appear good when compared to a few limited
416 observations, but an overall assessment is still not ready yet due to lack of
417 observations. This is to be reported in our future work.

418

419 **Acknowledgements** This work was jointly supported by the MOST of China (Grant
420 No. 2011CB403505 & 2014CB953904), the Strategic Priority Research Program of
421 the Chinese Academy of Sciences (Grant No. XDA01020304), Chinese Academy of

422 Sciences through the project KZCX2-EW-208, National Natural Science Foundation
423 of China (Grants No. 41376021), the Hundred Talent Program of the Chinese
424 Academy of Sciences, and Guangdong Marine disaster emergency response
425 technology research center (2012A032100004).

426 **Reference**

- 427 Bender, M. A., I. Ginis, R. Tuleya, B. Thomas, and T. Marchok, 2007: The operational GFDL
428 coupled hurricane–ocean prediction system& a summary of its performance. *Mon. Wea. Rev.*,
429 **135**, 3965–3989.
- 430 Blumberg, A. F. and G. L. Mellor, 1987: A description of a three-dimensional coastal ocean
431 circulation model. *Three Dimensional Coastal Ocean Models*, N. Heaps Ed., vol. 4.
432 American Geophysical Union, Washington, DC, 1-208.
- 433 Du, Y., and T. Qu, 2010: Three inflow pathways of the Indonesian throughflow as seen from the
434 simple ocean data assimilation. *Dyn. Atmos. Oceans*, doi:10.1016/j.dynatmoce.2010.04.001.
- 435 Dudhia, J., 1989: Numerical study of convection observed during the winter monsoon experiment
436 using a mesoscale two-dimensional model, *J. Atmos. Sci.*, **46**, 3077–3107.
- 437 Ferrier, B. S., Y. Lin, T. Black, E. Rogers, and G. DiMego, 2002: Implementation of a new
438 grid-scale cloud and precipitation scheme in the NCEP Eta model. Preprints, *15th Conf. on*
439 *Numerical Weather Prediction*, San Antonio, TX, Amer. Meteor. Soc., 280-283.
- 440 Fraedrich, K. and M. Leslie, 1989: Estimates of cyclone track predictability. I: Tropical cyclones
441 in the Australian region. *Quart. J. Roy. Meteor. Soc.* **115**, 79–92.
- 442 Giorgi, F., 2006: Regional climate modeling: Status and perspectives, *J. Phys. IV France*, **139**,
443 101-118.
- 444 Hong, S.-Y., Y. Noh, and J. Dudhia, 2006: A new vertical diffusion package with an explicit
445 treatment of entrainment processes. *Mon. Wea. Rev.*, **134**, 2318–2341.
- 446 Kanada1, S., A. Wada, M. Nakano, and T. Kato, 2012: Effect of planetary boundary layer schemes
447 on the development of intense tropical cyclones using a cloud-resolving model. *J. Geophys.*
448 *Res.: Atmospheres.*, **117(D3)**, DOI: 10.1029/2011JD016582.
- 449 Kain, J. S. and J. M. Fritsch, 1990: A one-dimensional entraining/detraining plume model and its
450 application in convective parameterization. *J. Atmos. Sci.*, **47**, 2784–2802.
- 451 Kain, J. S. and J. M. Fritsch, 1993: Convective parameterization for mesoscale models: The
452 Kain–Fritsch scheme. *The representation of cumulus convection in numerical models*,
453 Emanuel K. A. and Raymond D. J. Ed., No. 46, Meteorol. Monogr., Amer. Meteorol. Soc.,
454 165–170.
- 455 Kepert, J. D., 2012: Choosing a Boundary Layer Parameterization for Tropical Cyclone Modeling.
456 *Mon. Wea. Rev.*, **140**, 1427–1445.
- 457 Khain, A. and B. Lynn, 2011: Simulation of Tropical Cyclones Using Spectral Bin
458 Microphysics, Recent Hurricane Research - Climate, Dynamics, and Societal Impacts, Prof.
459 Anthony Lupo (Ed.), ISBN: 978- 953-307-238-8, InTech.
- 460 Kurihara, Y., M. A. Bender, T. E. Tuleya, and R. J. Ross, 1995: Improvements in the GFDL
461 hurricane prediction system. *Mon. Wea. Rev.*, **123**, 2791–2801.
- 462 Landman, W. A., A. Seth, and S. J. Camargo, 2005: The effect of regional climate model domain
463 choice on the simulation of tropical cyclone-like vortices in the Southwestern Indian Ocean, *J.*
464 *Climate*, **18**, 1263-1274.
- 465 Leslie, L. M. et al., 1998: Improved hurricane track forecasting from the continuous assimilation
466 of high quality satellite wind data. *Mon. Wea. Rev.*, **126**, 1248–1257.
- 467 Li, Y., S. Peng, J. Yan, and L. Xie, 2013: On improving storm surge forecasting using an adjoint
468 optimal technique. *Ocean Modell.*, **72**, 185–197.
- 469 Liu, D. F., L. Pang, and B. T. Xie, 2009: Typhoon disaster in China: prediction, prevention, and

470 mitigation. *Nat Hazards*, **49**, 421–436.

471 Lo, J. C. F., Z. L. Yang, R. A., and Pielke Sr., 2008: Assessment of three dynamical climate
472 downscaling methods using the weather research and forecasting (WRF) model. *J. Geophys.*
473 *Res.* **113**: D09112. doi: 10.1029/2007JD009216.

474 Mellor, G. L., 2003: *Users guide for a three-dimensional, primitive equation, numerical ocean*
475 *model (June 2003 version)*, Atmos. and Ocean. Sci., Princeton University, 53 pp.

476 Mellor, G. L., and T. Yamada, 1982: Development of a turbulence closure model for geophysical
477 fluid problems. *Rev. Geophys. Space Phys.*, **20**, 851–875.

478 Michalakes, J. G., J. Dudhia, D. Gill, J. Klemp, and W. Skamarock, 1998: Design of a next
479 generation regional weather research and forecast model. *River Edge, New Jersey: Towards*
480 *Teracomputing*, World Scientific, 117–124.

481 Mlawer, E. J., S. J. Taubman, P. D. Brown, M. J. Iacono, and S. A. Clough, 1997: Radiative
482 transfer for inhomogeneous atmosphere: RRTM, a validated correlated-k model for the
483 longwave. *J. Geophys. Res.*, **102** (D14), 16663–16682.

484 Neumann, C. J., and J. M. Pelissier, 1981: An analysis of Atlantic tropical cyclone forecast errors,
485 1970–1979. *Mon. Wea. Rev.*, **109**, 1248–1266.

486 Pattanayak, S., U. C. Mohanty, and K. K. Osuri, 2012: Impact of Parameterization of Physical
487 Processes on Simulation of Track and Intensity of Tropical Cyclone Nargis (2008) with
488 WRF-NMM Model. *The Scientific World Journal*, 2012, Article ID 671437.

489 Peng, M., L. Xie, and L. J. Pietrafesa, 2005: A numerical study on hurricane induced storm surge
490 and inundation in Charleston Harbor, South Carolina. *J. Geophys. Res.* **111**, C08017.
491 <http://dx.doi.org/10.1029/2004JC002755>.

492 Peng, S., L. Xie, B. Liu, and F. Semazzi, 2010: Application of Scale-Selective Data Assimilation
493 to Regional Climate Modeling and Prediction. *Mon. Wea. Rev.*, **138**, 1307-1318.

494 Peng, S., Y.-K. Qian, Z. Lai, S. Hao, S. Chen, H. Xu, D. Wang, X. Xu, J. C. L. Chan, H. Zhou, D.
495 Liu , 2014: On the mechanisms of the recurvature of super typhoon Megi. *Scientific Reports*,
496 **4**, 4451 | DOI: 10.1038/srep04451.

497 Powell, M. D., and S. D. Aberson, 2001: Accuracy of United States tropical cyclone landfall
498 forecasts in the Atlantic basin (1976–2000). *Bull. Amer. Meteor. Soc.*, **82**, 2749–2768.

499 Plu, M., 2011: A new assessment of the predictability of tropical cyclone tracks. *Mon. Wea. Rev.*,
500 **139**, 3600–3608.

501 Qu, T., Y. Du, G. Meyers, A. Ishida, and D. Wang, 2005: Connecting the tropical Pacific with
502 Indian Ocean through South China Sea. *Geophys. Res. Lett.*, **32**, L24609, doi,
503 10.1029/2005GL024698.

504 Qu, T., and Y. Du, 2006: South China Sea Throughflow: A heat and freshwater conveyor in the
505 Maritime Continent. *Geophys. Res. Lett.*, **33**, L23617, doi, 10.1029/2006GL028350.

506 Rao, D. V. B. and D. H. Prasad, 2007: Sensitivity of tropical cyclone intensification to boundary
507 layer and convective processes. *Natural Hazards*, **41**, 429-445.

508 Skamarock, W. C., J. B. Klemp, J. Dudhia, D. O. Gill, D. M. Barker, M. G. Duda, X. Huang, W.
509 Wang, and J. G. Powers, 2008: *A Description of the Advanced Research WRF Version 3*, 113
510 pp. Available at http://www.mmm.ucar.edu/wrf/users/docs/arw_v3.pdf

511 Tallapragada, V., L. Bernardet., Gopalakrishnan, S., Y Kwon, Q.L. Liu, T. Marchok, , M. Tong, R.
512 Tuleya, R. Yablonsky, and X. Zhang, 2013: Hurricane Weather Research and Forecasting

513 (HWRf) Model: 2013 Scientific Documentation. *NCAR Development Tested Bed Center*
514 *Report*.

515 Tolman, H. L., 1997: A New Global Wave Forecast System at NECP. *Ocean Wave Measurements*
516 *and Analysis*, B. L. Edge and J. M. Helmsley Ed., Vol. 2, ASCE, 777-786.

517 Tolman, H. L., 1999: *User Manual and System Documentation of WAVEWATCH-III version 1.18*.
518 Technical Note, 110 pp.

519 Tolman, H. L., 2002: *User manual and system documentation of WAVEWATCH-III version 2.22*.
520 Technical Note, U.S. Department of Commerce, NOAA, NWS, NCEP, Washington, DC.

521 Wang, D., Q. Liu, R.X. Huang, Y. Du, and T. Qu, 2006: Interannual variability of the South China
522 Sea throughflow inferred from wind data and an ocean data assimilation product. *Geophys.*
523 *Res. Lett.* **33**, L14605, doi, 10.1029/2006GL026316.

524 Weisberg, R.H., Zheng, L.Y., 2008: Hurricane storm surge simulations comparing
525 three-dimensional with two-dimensional formulations based on an Ivan-like storm over the
526 Tampa Bay, Florida region. *J. Geophys. Res.* **113**, C12001.
527 <http://dx.doi.org/10.1029/2008JC005115>.

528 Wu, C.-C. and Kuo, Y.-H., 1999: Typhoons Affecting Taiwan: Current Understanding and Future
529 Challenges. *Bull. Am. Meteorol. Soc.* **80**, 67-80.

530 Xie, L., Pietrafesa, L.J., Peng, M., 2004. Incorporation of a mass-conserving inundation scheme
531 into a three-dimensional storm surge model. *J. Coastal Res.* **20**, 1209–1223.

532 Xie, L., B. Liu, and S. Peng, 2010: Application of scale-selective data assimilation to tropical
533 cyclone track simulation. *J. Geophys. Res.*, **115**, D17105, doi:10.1029/2009JD013471.

534 Zhang, Y., V. Duliere, P. Mote, and E. P. Salathe Jr., 2009: Evaluation of WRF and HadRM
535 mesoscale climate simulations over the United States Pacific Northwest. *J. Climate.* **22**,
536 5511–5526

537 Zhou, H., W. Zhu, and S. Peng, 2013: The impacts of different micro-physics schemes and
538 boundary layer schemes on the simulated track and intensity of super typhoon Megi (1013), *J.*
539 *Tropical Meteor.*, **28**(4), 599-608. (in Chinese)

540

541 **Figure captions**

542 Fig. 1 The flow chart for the system of EPMEF. Here the ‘OPTS’ means the ‘Tidal
543 Data Prediction Software’.

544 Fig. 2 The model domains of WRF and the JTWC “best” tracks of 18 tropical cyclones
545 of 2013 that entered the inner domain with life cycle longer than 48 hours and were
546 forecasted by at least 4 agencies (of JTWC, JMA, NMCC, CWBT, NCEP and
547 EPMEF).

548 Fig. 3 The mean track position errors (TPE, unit: km) and the relative errors with their
549 standard deviations (black vertical lines) of the predicted track for the 10 tropical
550 cyclones in 2011 from different agencies for (a) 24-h, (b) 48-h, and (c) 72-h forecasts,
551 respectively. Here JTWC denotes the U.S. Navy/Air Force Joint Typhoon Warning
552 Center, JMA the Japan Meteorological Administration, NMCC the National
553 Meteorological Center of China, and CWBT the Central Weather Bureau of Taiwan
554 (CWBT).

555 Fig. 4 The same as Fig. 3, except for the 16 tropical cyclones in 2012 with an
556 additional agency NCEP and hindcast EPMEF-6. The Environmental Modelling
557 Center (EMC) of the National Center of Environment Prediction (NCEP) in U.S.
558 began to make real-time forecasts for West Pacific TCs using HWRF model since
559 2012 TC season. EPMEF-6 is the same as EPMEF except that EPMEF-6 used the
560 GFS forecasts of the previous cycle (6-h early).

561 Fig. 5 The same as Fig. 3, except for the 18 tropical cyclones in 2013 with an
562 additional agency NCEP. The Environmental Modelling Center (EMC) of the

563 National Center of Environment Prediction (NCEP) in U.S. began to make real-time
564 forecasts for West Pacific TCs using HWRF model since 2012 TC season.

565 Fig. 6 The track position errors (TPE, unit: km) of Nanmadul (2011) from different
566 agencies for multiple (a) 24-h forecast, (b) 48-h forecast and (c) 72-h forecast
567 initializing every 6 hours starting at 0000 UTC 24 Aug. 2011 (the interval of abscissa
568 is 6 hours), and (d) the “best” and predicted tracks of Nanmadul (2011) from different
569 agencies for a single 72-h forecast initializing at 1200 UTC 27 Aug. 2011.

570 Fig. 7 The track position errors (TPE, unit: km) of Rumbia (2013) from different
571 agencies for multiple (a) 24-h forecast, (b) 48-h forecast and (c) 72-h forecast
572 initializing every 6 hours starting at 1200 UTC 28 Jun. 2013 (the interval of abscissa
573 is 6 hours), and (d) the “best” and predicted tracks of Rumbia (2013) from different
574 agencies for a single 72-h forecast initializing at 0000 UTC 29 Jun. 2013.

575 Fig. 8 The same as Fig. 6, except for Nesat (2011) from different agencies for multiple
576 (a) 24-h forecast, (b) 48-h forecast and (c) 72-h forecast initializing every 6 hours
577 starting at 0000 UTC 24 Sep. 2011, and (d) the “best” and predicted tracks o
578 initializing at 1200 UTC 25 Aug. 2011.

579 Fig. 9 The “best” track and the predicted tracks for a single 72-h forecast from
580 different agencies for (a) Megi (2010) initializing at 0000 UTC 18 Oct. 2010 and (b)
581 Roke (2011) initializing eat 0600 UTC 14 Sep. 2011, and the track position errors
582 (TPE, unit: km) of Roke (2011) from different agencies for (c) 48-h forecast and (d)
583 72-h forecast initializing every 6 hours starting at 1800 UTC 13 Sep. 2011 (the
584 interval of abscissa is 6 hours).

585 Fig. 10 The steering flows and the 500-hPa geopotential height (unit: geopotential
586 meter, GPM) from (a), (c) the “late model” and (b), (d) the “early model” at (a), (b)
587 the initialization time of 1200 UTC 3 Oct. 2012 and (c), (d) the 30-h forecast time
588 valid at 1800 UTC 4 Oct. 2012 for the typhoon Gaemi (2012), imposed by the “best”
589 (black) and simulated (red) tracks as well as the vectors of steering flows at the
590 corresponding time.

591 Fig. 11 The mean biases of (a) u-components and (b) v-components of steering flows
592 from the 72-h forecasts of EPMEF and EPMEF-6 against the FNL analysis averaged
593 over an ensemble of model runs initialized at every 6-h from 0000 UTC 2 Oct. to
594 1200 UTC 5 Oct. for the typhoon Gaemi (2012).

595 Fig. 12 The mean biases of (a) u-components and (b) v-components of steering flows
596 from the 72-h forecasts by different combinations of 4 microphysics schemes (Ferrier,
597 Goddard, WSM6, Lin) and three PBL schemes (YSU, MYJ, MYNN2) against the
598 FNL analysis for typhoon Vicente (2012), which are averaged over an ensemble of
599 model runs initialized at every 6-h from 1200 UTC 21 Jul. to 1800 UTC 23 Jul..

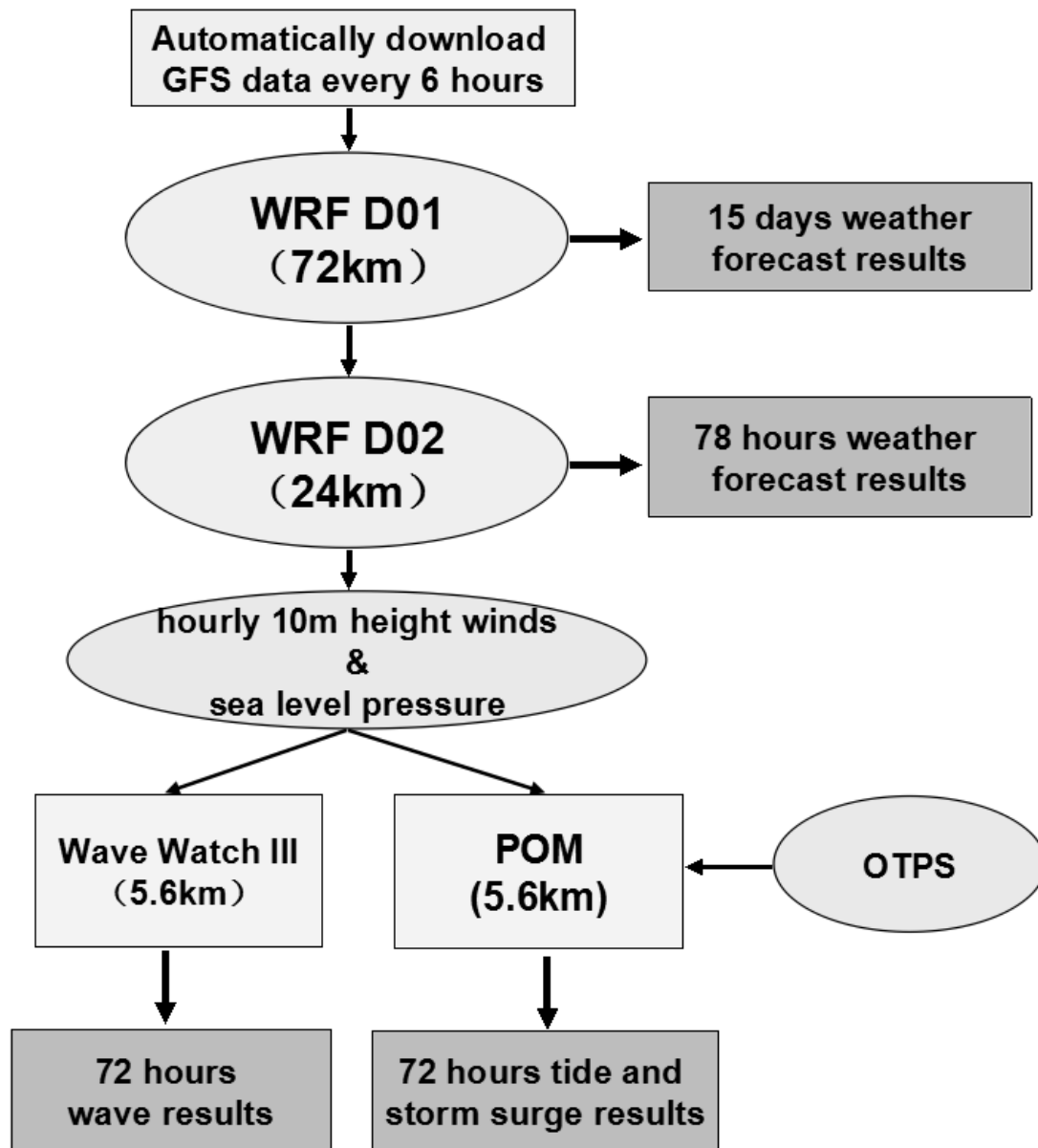
600

601 **Table 1.** The mean track position errors (TPE, unit: km) and relative errors (indicated
602 in blanket) of 24-h, 48-h and 72-h forecasts as well as the total rank for different
603 combinations of four microphysics schemes and three PBL schemes, averaged over an
604 ensemble of forecasts initializing at every 6 hours from 1200 UTC 21 Jul. to 1800
605 UTC 23 Jul. for typhoon Vicente (2012).

		Ferrier	Goddard	WSM6	Lin
24h fcst	YSU	69.9 (0.80)	81.7 (0.93)	84.8 (0.97)	88.0 (1.01)
	MYJ	94.6 (1.08)	90.1 (1.03)	87.4 (1.00)	93.5 (1.07)
	MYNN2	83.5 (0.95)	84.3 (0.96)	96.9 (1.11)	95.2 (1.09)
48h fcst	YSU	156.2 (0.94)	184.0 (1.10)	170.5 (1.02)	171.1 (1.02)
	MYJ	144.0 (0.86)	149.8 (0.90)	142.4 (0.85)	157.3 (0.94)
	MYNN2	185.0 (1.11)	176.9 (1.06)	188.0 (1.13)	178.8 (1.07)
72h fcst	YSU	134.5 (0.50)	330.3 (1.22)	325.9 (1.21)	444.2 (1.64)
	MYJ	--- (---)	--- (---)	--- (---)	--- (---)
	MYNN2	182.5 (0.68)	235.2 (0.87)	228.9 (0.85)	280.7 (1.04)
RANK (SUM)	YSU	1 (2.23)	7 (3.26)	5 (3.20)	8 (3.67)
	MYJ	9 (---)	9 (---)	9 (---)	9 (---)
	MYNN2	2 (2.74)	3 (2.89)	4 (3.10)	6 (3.20)

606

607

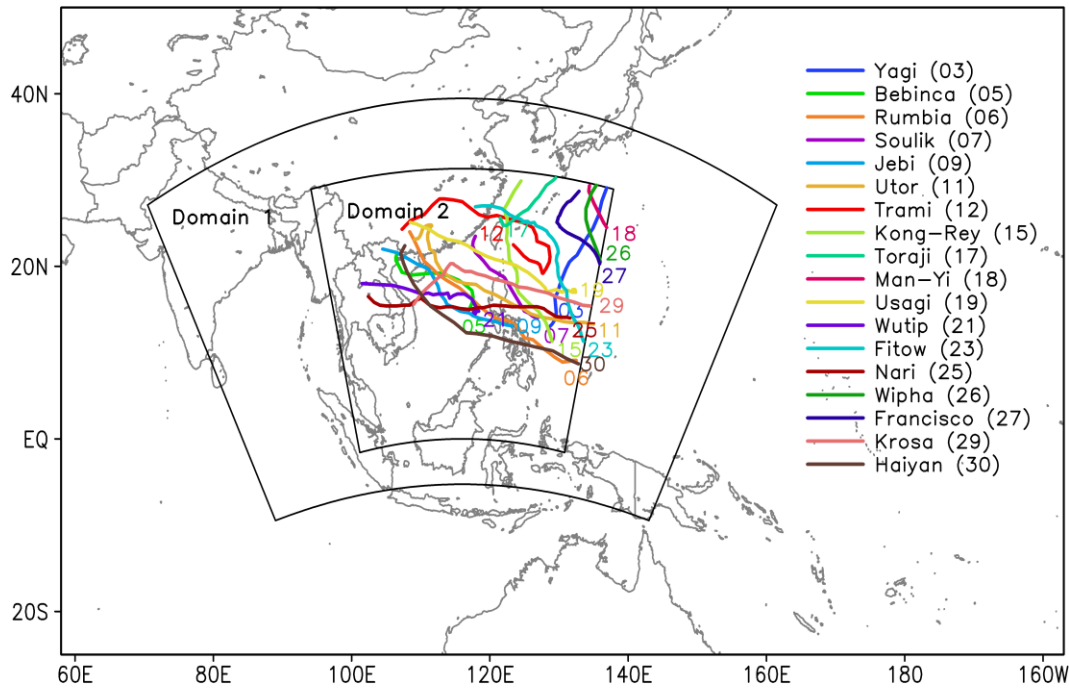


608

609 Fig. 1 The flow chart for the system of EPMEF. Here the 'OPTS' means the 'Tidal

610 Data Prediction Software'.

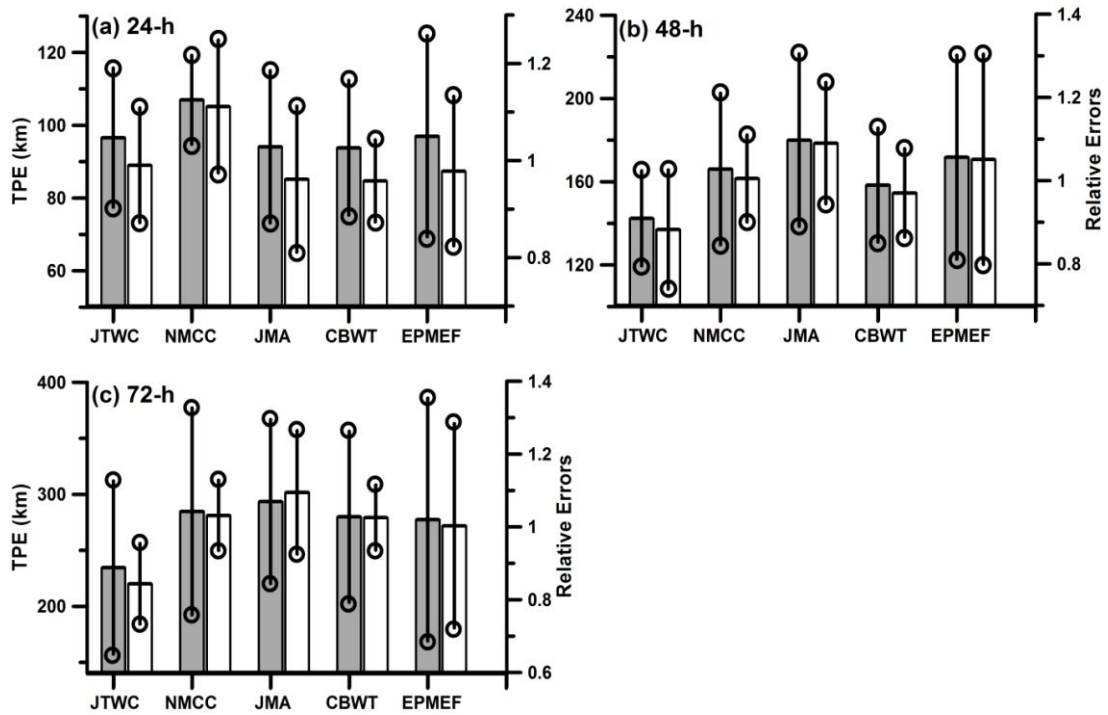
611



612

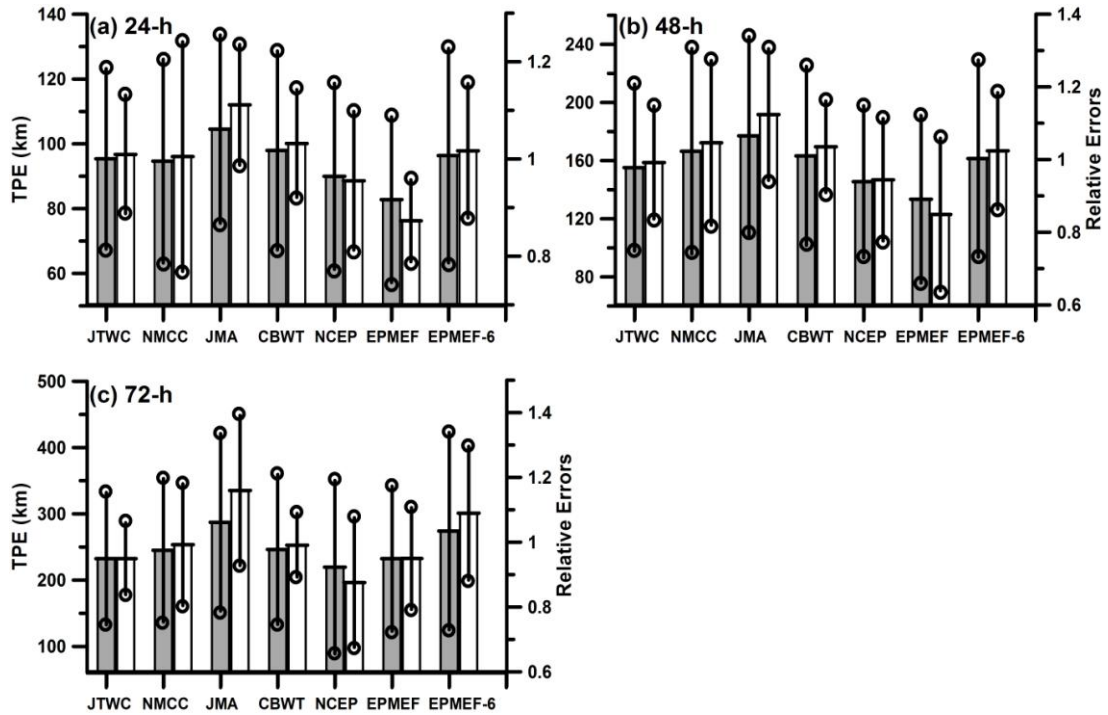
613 Fig. 2 The model domains of WRF and the JTWC “best” tracks of 18 tropical cyclones
 614 of 2013 that entered the inner domain with life cycle longer than 48 hours and were
 615 forecasted by at least 4 agencies (of JTWC, JMA, NMCC, CWBT, NCEP and
 616 EPMEF).

617



618

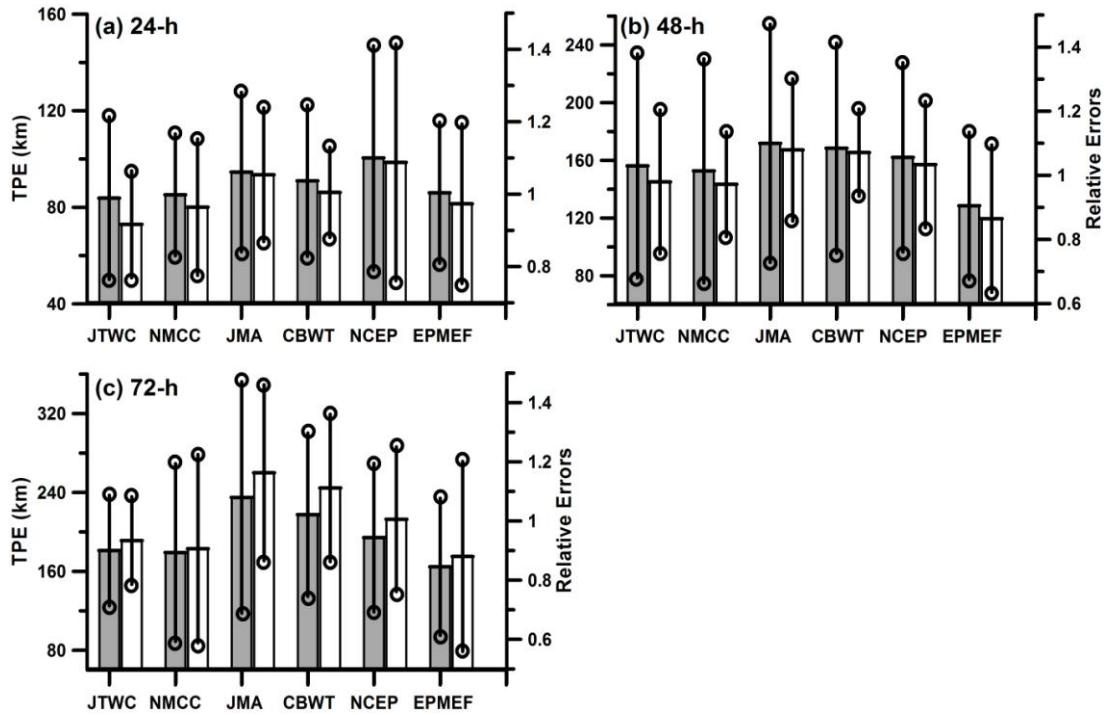
619 Fig. 3 The mean track position errors (TPE, unit: km) and the relative errors with their
 620 standard deviations (black vertical lines) of the predicted track for the 10 tropical
 621 cyclones in 2011 from different agencies for (a) 24-h, (b) 48-h, and (c) 72-h forecasts,
 622 respectively. Here JTWC denotes the U.S. Navy/Air Force Joint Typhoon Warning
 623 Center, JMA the Japan Meteorological Administration, NMCC the National
 624 Meteorological Center of China, and CWBT the Central Weather Bureau of Taiwan
 625 (CWBT).



626

627 Fig. 4 The same as Fig. 3, except for the 16 tropical cyclones in 2012 with an
 628 additional agency NCEP and hindcast EPMEF-6. The Environmental Modelling
 629 Center (EMC) of the National Center of Environment Prediction (NCEP) in U.S.
 630 began to make real-time forecasts for West Pacific TCs using HWRF model since
 631 2012 TC season. EPMEF-6 is the same as EPMEF except that EPMEF-6 used the
 632 GFS forecasts of the previous cycle (6-h early).

633

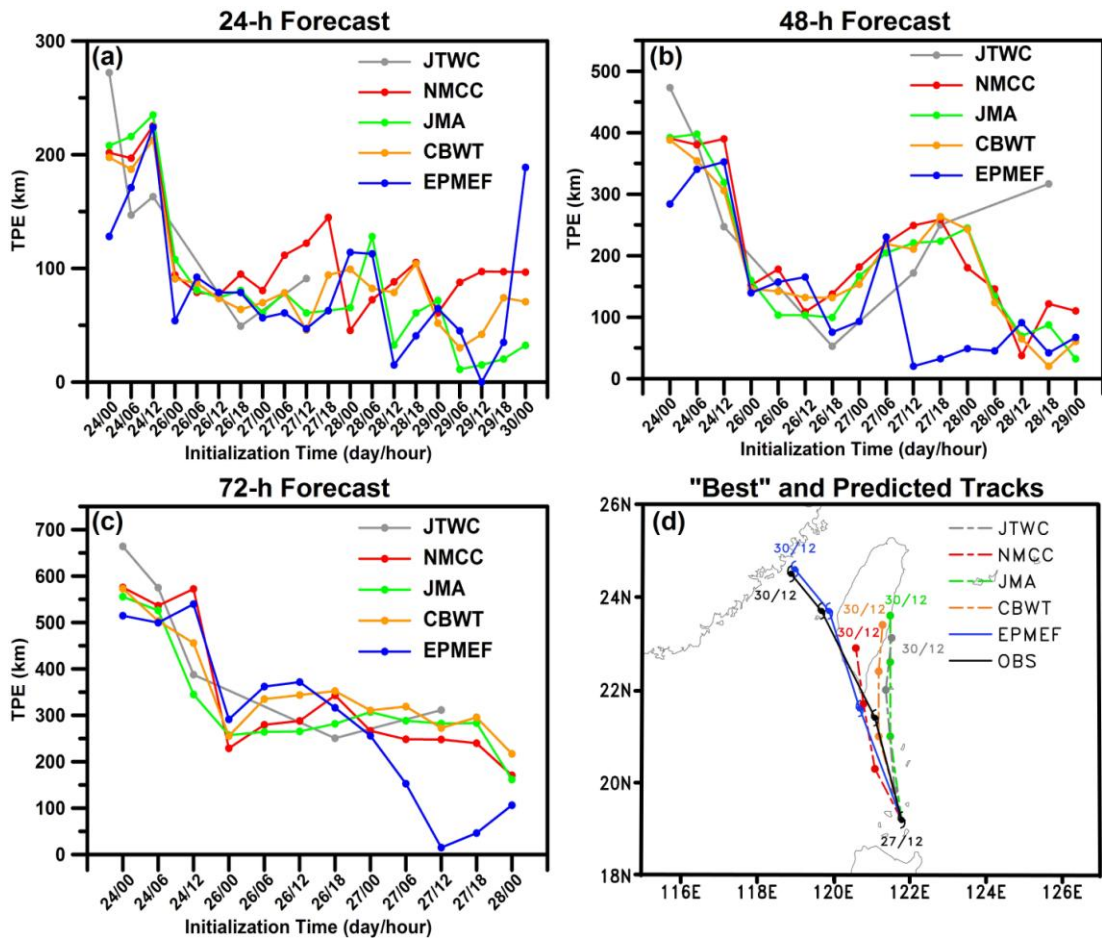


634

635 Fig. 5 The same as Fig. 3, except for the 18 tropical cyclones in 2013 with an
 636 additional agency NCEP. The Environmental Modelling Center (EMC) of the
 637 National Center of Environment Prediction (NCEP) in U.S. began to make real-time
 638 forecasts for West Pacific TCs using HWRF model since 2012 TC season.

639

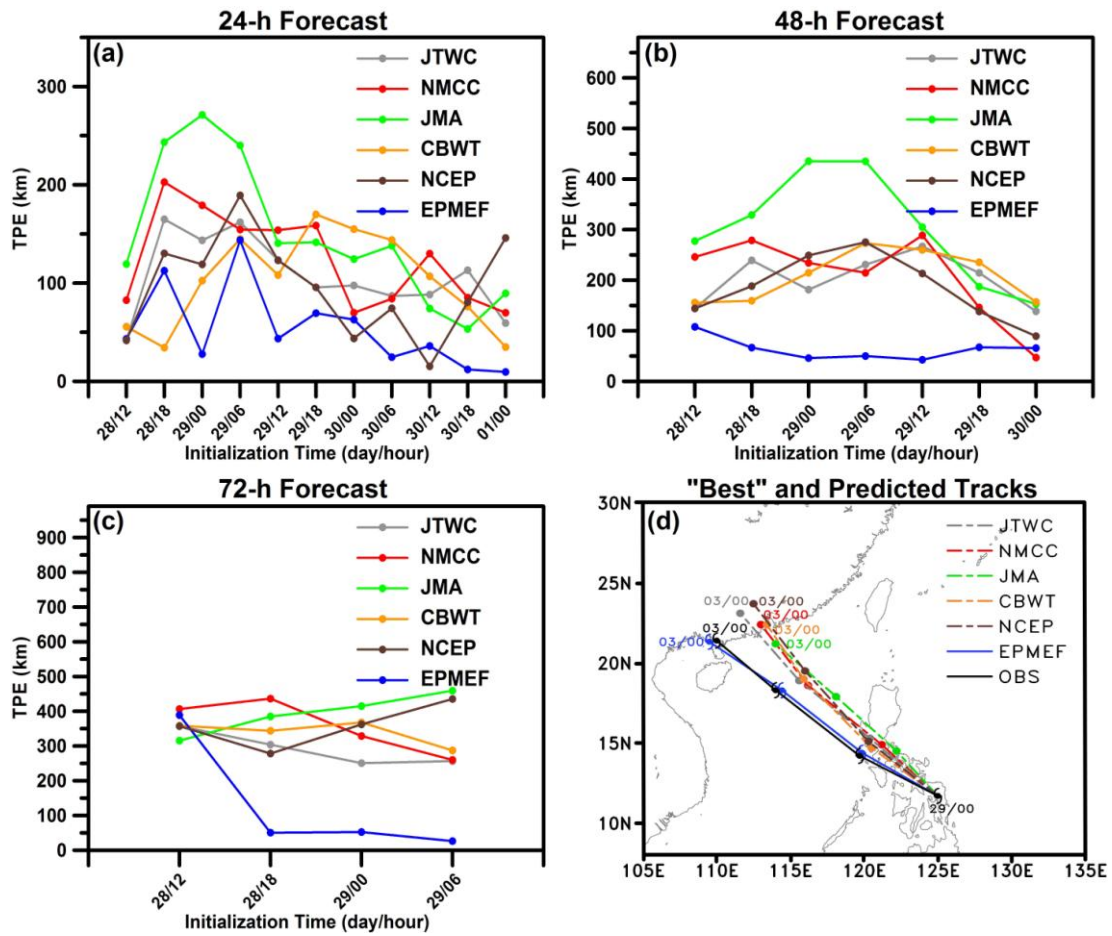
640



642

643 Fig. 6 The track position errors (TPE, unit: km) of Nanmadul (2011) from different
 644 agencies for multiple (a) 24-h forecast, (b) 48-h forecast and (c) 72-h forecast
 645 initializing every 6 hours starting at 0000 UTC 24 Aug. 2011 (the interval of abscissa
 646 is 6 hours), and (d) the “best” and predicted tracks of Nanmadul (2011) from different
 647 agencies for a single 72-h forecast initializing at 1200 UTC 27 Aug. 2011.

648

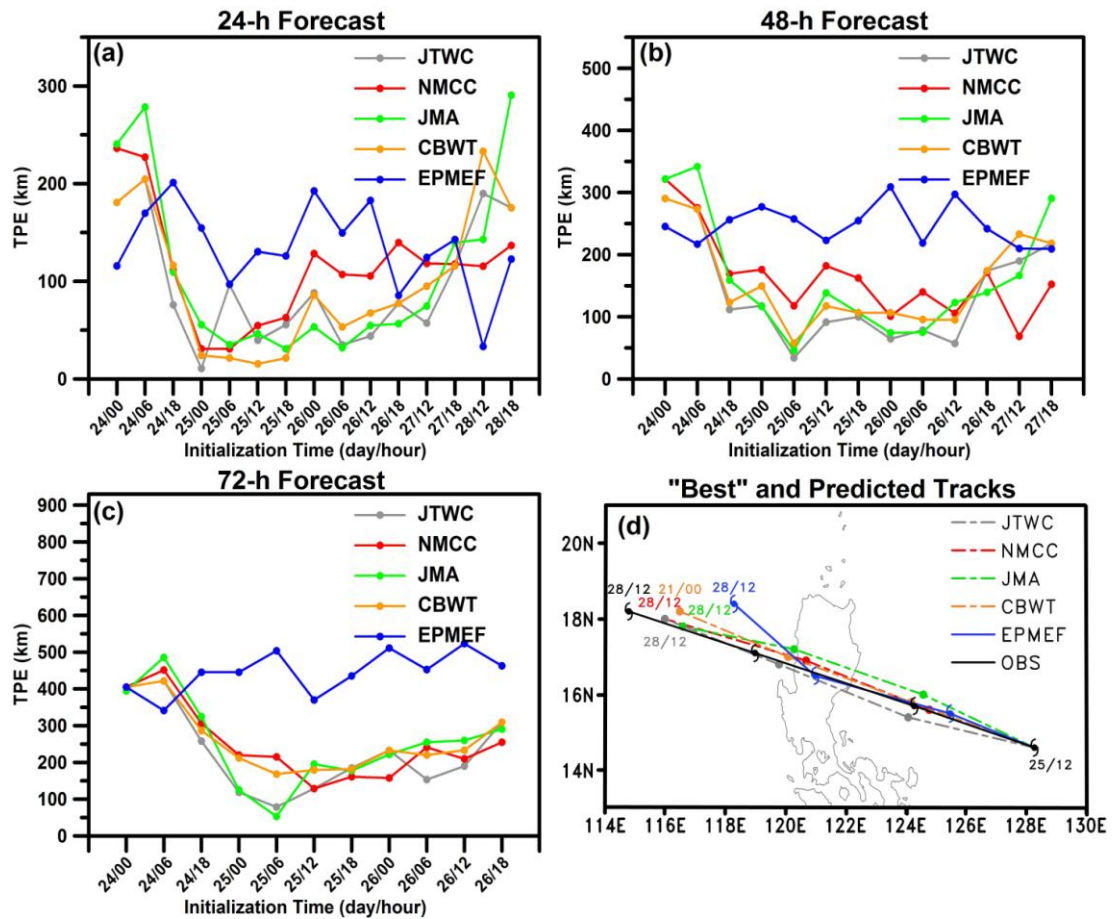


650

651 Fig. 7 The track position errors (TPE, unit: km) of Rumbia (2013) from different
 652 agencies for multiple (a) 24-h forecast, (b) 48-h forecast and (c) 72-h forecast
 653 initializing every 6 hours starting at 1200 UTC 28 Jun. 2013 (the interval of abscissa
 654 is 6 hours), and (d) the “best” and predicted tracks of Rumbia (2013) from different
 655 agencies for a single 72-h forecast initializing at 0000 UTC 29 Jun. 2013.

656

657



658

659 Fig. 8 The same as Fig. 6, except for Nesat (2011) from different agencies for multiple

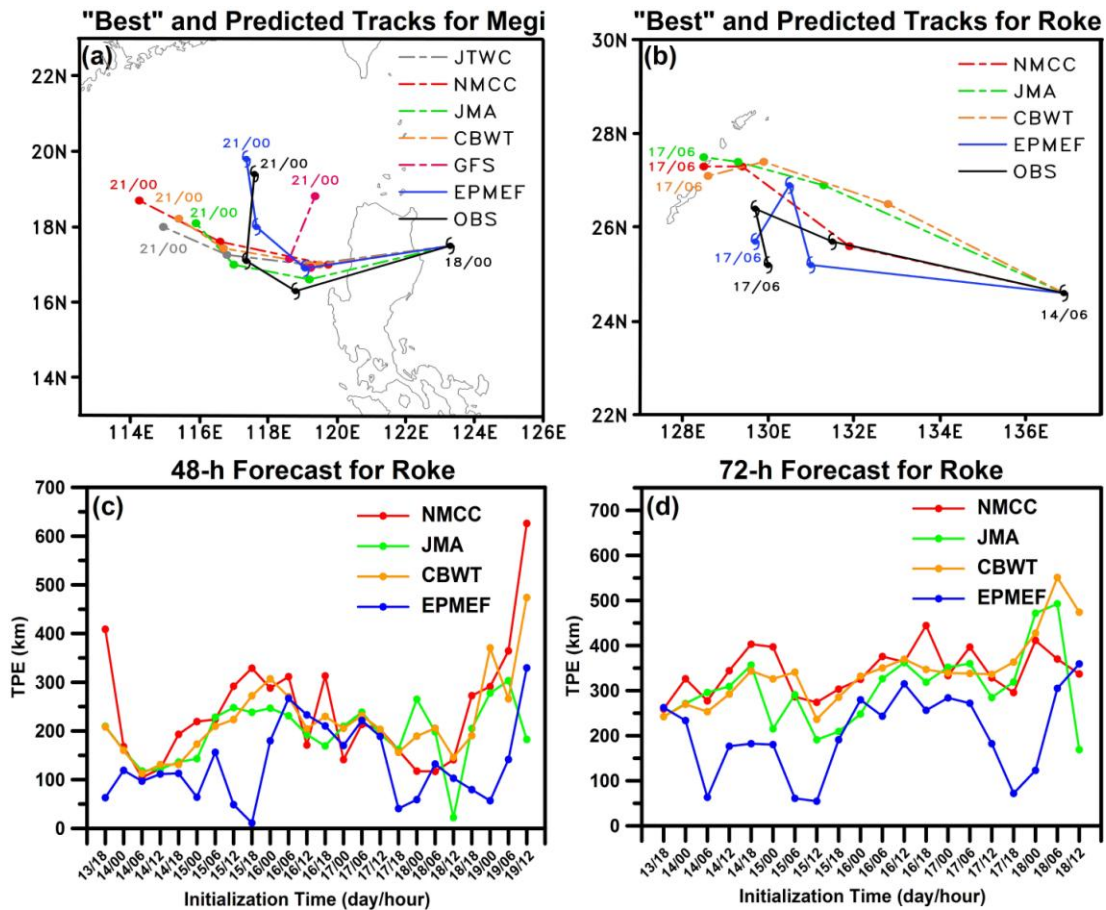
660 (a) 24-h forecast, (b) 48-h forecast and (c) 72-h forecast initializing every 6 hours

661 starting at 0000 UTC 24 Sep. 2011, and (d) the "best" and predicted tracks o

662 initializing at 1200 UTC 25 Aug. 2011.

663

664



665

666 Fig. 9 The “best” track and the predicted tracks for a single 72-h forecast from

667 different agencies for (a) Megi (2010) initializing at 0000 UTC 18 Oct. 2010 and (b)

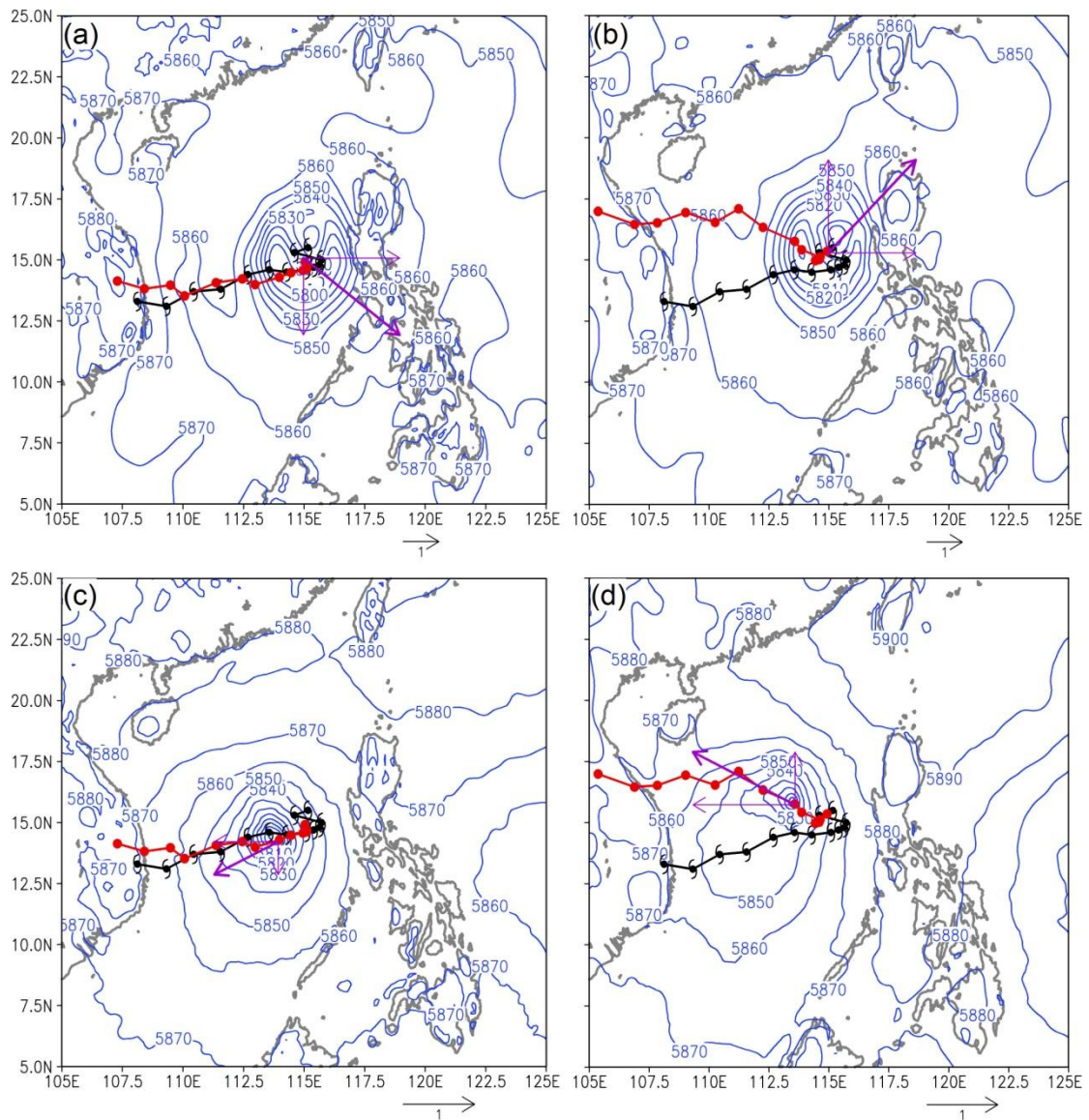
668 Roke (2011) initializing at 0600 UTC 14 Sep. 2011, and the track position errors

669 (TPE, unit: km) of Roke (2011) from different agencies for (c) 48-h forecast and (d)

670 72-h forecast initializing every 6 hours starting at 1800 UTC 13 Sep. 2011 (the

671 interval of abscissa is 6 hours).

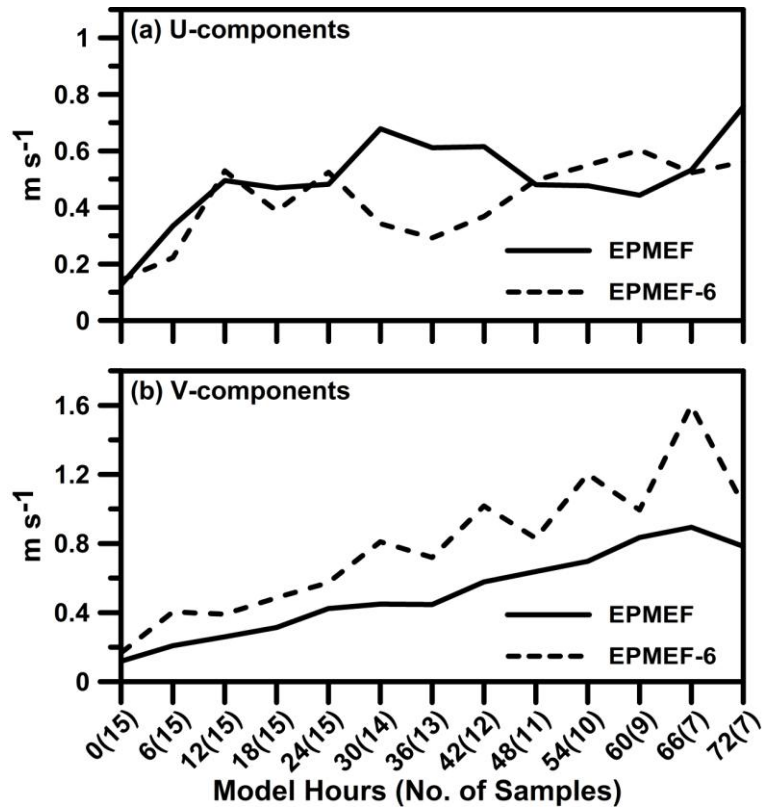
672



673

674 Fig. 10 The steering flows and the 500-hPa geopotential height (unit: geopotential
 675 meter, GPM) from (a), (c) the “late model” and (b), (d) the “early model” at (a), (b)
 676 the initialization time of 1200 UTC 3 Oct. 2012 and (c), (d) the 30-h forecast time
 677 valid at 1800 UTC 4 Oct. 2012 for the typhoon Gaemi (2012), imposed by the “best”
 678 (black) and simulated (red) tracks as well as the vectors of steering flows at the
 679 corresponding time.

680

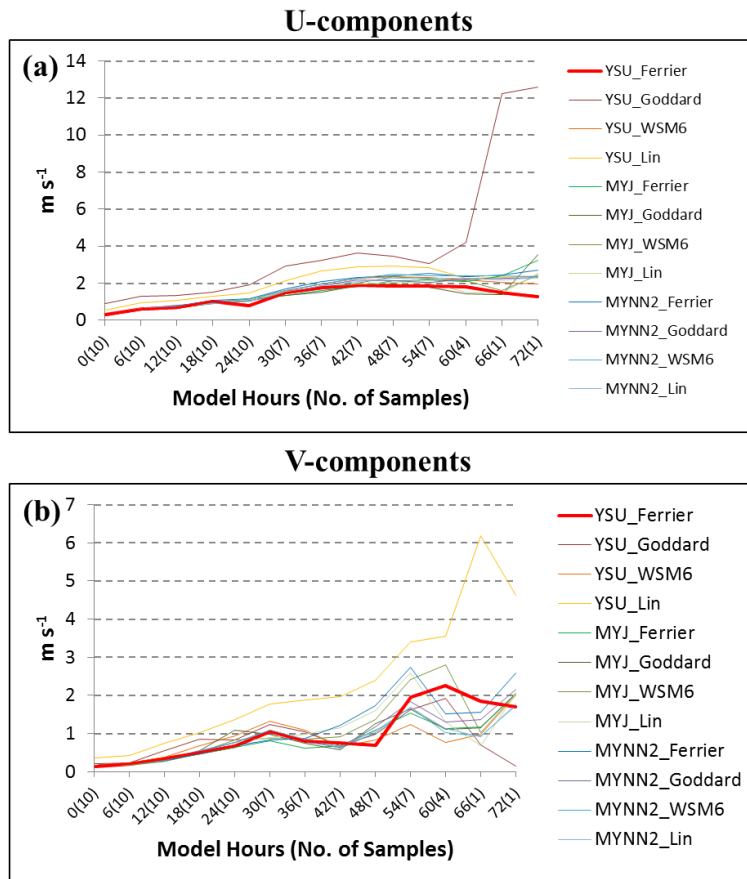


681

682 Fig. 11 The mean biases of (a) u-components and (b) v-components of steering flows
 683 from the 72-h forecasts of EPMEF and EPMEF-6 against the FNL analysis averaged
 684 over an ensemble of model runs initialized at every 6-h from 0000 UTC 2 Oct. to
 685 1200 UTC 5 Oct. for the typhoon Gaemi (2012).

686

687



688

689 Fig. 12 The mean biases of (a) and (b) v-components of steering flows from the 72-h
 690 forecasts by different combinations of 4 microphysics schemes (Ferrier, Goddard,
 691 WSM6, Lin) and three PBL schemes (YSU, MYJ, MYNN2) against the FNL analysis
 692 for typhoon Vicente (2012), which are averaged over an ensemble of model runs
 693 initialized at every 6-h from 1200 UTC 21 Jul. to 1800 UTC 23 Jul..